Nearest-Neighbor Configuration in (GaIn)(NAs) Probed by X-Ray Absorption Spectroscopy

Vincenzo Lordi,[1,*] Vincent Gambin,[1] Stephan Friedrich,[2,†] Tobias Funk,[2] Toshiyuki Takizawa,[3]
Kazuyuki Uno,[4] and James S. Harris[1]

[1]*Solid State and Photonics Laboratory, Stanford University, Stanford, California 94305*
[2]*Lawrence Berkeley National Laboratory, Berkeley, California 94720*
[3]*Matsushita Electric Industrial Co., Ltd., Osaka, Japan*
[4]*Wakayama University, Wakayama, Japan*
(Received 18 November 2002; published 11 April 2003)

$Ga_{1-x}In_xN_yAs_{1-y}$ is a promising material system for the fabrication of inexpensive "last-mile" optoelectronic components. However, details of its atomic arrangement and the relationship to observed optical properties is not fully known. Particularly, a blueshift of emission wavelength is observed after annealing. In this work, we use x-ray absorption fine structure to study the chemical environment around N atoms in the material before and after annealing. We find that as-grown molecular beam epitaxy material consists of a nearly random distribution of atoms, while postannealed material shows segregation of In toward N. *Ab initio* simulations show that this short-range ordering creates a more thermodynamically stable alloy and is responsible for blueshifting the emission.

DOI: 10.1103/PhysRevLett.90.145505 PACS numbers: 61.10.Ht, 71.15.Mb, 81.05.Ea, 81.40.Tv

The astonishing growth of the Internet and data transmission volume in recent years is resulting in increased bandwidth requirements for fiber-optic networks, especially at the metro-area (MAN) and local-area (LAN) levels. The lack of low-cost, high-speed optoelectronic components for MANs and LANs introduces severe bottlenecks in the overall network. New materials and architectures are required to solve this problem. $Ga_{1-x}In_xN_yAs_{1-y}$ [1] is a promising material system for enabling the fabrication of low-cost components on GaAs operating at the communications wavelengths of 1.3–1.55 μm, such as vertical-cavity surface-emitting lasers [2]. The addition of small amounts of N to GaAs has the remarkable effect of sharply lowering the band gap, an effect that was unexpected due to the greater band gap of GaN relative to GaAs. The addition of In allows the lattice constant to be closely matched to GaAs for epitaxial growth, while further reducing the band gap.

As-grown GaInNAs quantum wells generally exhibit inefficient photoluminescence (PL). Rapid thermal annealing (RTA) at ~720–850 °C for 1–2 min improves the PL efficiency dramatically, but also produces an undesirable blueshift in the peak emission wavelength [3,4]. Understanding the origin of the band gap shift and the mechanism of annealing is critical for successful engineering of the growth and processing of GaInNAs devices.

Theoretical studies have shown that the detailed atomic configuration in a semiconductor crystal can significantly affect its optical properties [5,6]. Previous studies on GaInNAs grown by organometallic vapor phase epitaxy have used photoreflectance in tandem with tight-binding calculations [7], and Fourier transform infrared spectroscopy on low In-content material [8] to examine N bonding. In this Letter, we show that the nearest neighbor (nn) configuration around N atoms in GaInNAs modulates the band gap and varies from a nearly random configuration at growth to a more thermodynamic distribution after RTA. The nn configuration was measured using x-ray absorption spectroscopy (XAS), both in the near-edge (x-ray absorption near-edge structure, or XANES) and extended-edge (extended x-ray absorption fine structure, or EXAFS) regions. Data analysis was assisted by *ab initio* computer simulations of the band structure. The observed change in N nn configuration toward increased N—In bonding is shown to be responsible for blueshifting the band gap after RTA.

$Ga_{1-x}In_xN_yAs_{1-y}$ alloys, with $x \sim 0.3$ and $y \sim 0.03$, were grown on GaAs substrates using solid-source molecular beam epitaxy (MBE) [4,9,10]. Atomic N was provided by a rf plasma cell at 250–300 W power and 0.1–0.5 sccm flow rate. A low substrate temperature of ~420 °C was used to inhibit phase segregation. GaNAs samples were also grown for reference.

Nitrogen *K*-edge XANES spectra were taken in fluorescence from both as-grown and annealed samples. The measurements were performed at beam line 4.0.2 of the Advanced Light Source using a high-resolution superconducting tunnel junction x-ray detector operated at ~0.1 K [11]. Indium *K*-edge EXAFS spectra were measured at beam line BL01B1 of SPring-8 using a liquid N_2-cooled Ge detector.

Ab initio calculations were performed using the Vienna *Ab Initio* Simulation Package [12], which is based on the Kohn-Sham density-functional theory using a plane-wave basis set. Ultrasoft Vanderbilt pseudopotentials [13] were employed, using the local density approximation for the exchange-correlation functional. The atomic potentials were generated using theoretical calculations on atoms, without fitting to experimental properties. Total energy calculations were used to determine equilibrium atomic configurations, while partial local

 © 2003 The American Physical Society

density of states (PLDOS) calculations were used to simulate XANES spectra. For total energy calculations, a $3 \times 3 \times 3$ Monkhorst-Pack **k**-point mesh [14] was used, while a $6 \times 6 \times 6$ mesh was used for PLDOS. Band structures were calculated using 51 **k** points. The basis set cutoff energy was 26–32 Ry. Supercells of 64 atoms were used to simulate $Ga_{1-x}In_xN_yAs_{1-y}$ with $x \sim 0.25$–0.30 (8–10 In atoms) and $y \sim 0.03$ (1 N atom).

GaInNAs is nominally a zinc-blende random alloy, with the Group III elements (Ga and In) sharing one fcc lattice and the Group V elements (As and N) occupying a second interpenetrating fcc lattice. Each N atom sits in the center of a tetrahedron, surrounded by a total of four Ga and/or In atoms, as shown in Fig. 1(a). If the arrangement of atoms in the alloy were random, the probability distribution for finding a given number of In atoms surrounding any Group V atom is shown in Fig. 1(b), for $x = 0.3$. In the following, we adopt the notation "$GaInNAs^{(n)}$" to denote a model crystal with n In nn's around each N atom (i.e., $GaInNAs^{(0)}$ indicates a crystal where every N atom is bonded to four Ga atoms).

The XAS experiments were motivated by atomic relaxation simulations that showed a decrease in total energy by > 10 kcal/mol when two or more In atoms are bonded to N, despite an increase in overall lattice constant leading to a slight increase in compressive strain energy when growing GaInNAs epitaxially on GaAs [see Fig. 1(c)]. The decrease in chemical energy with increasing number of N—In bonds is due to overall decreases in individual bond strains, since the longer N—In bond is stretched less from equilibrium than the N—Ga bond. Furthermore, band structure calculations show an increase in band gap of $\sim$150 meV for the thermodynamically favored $GaInNAs^{(3)}$ over $GaInNAs^{(0)}$, consistent with the observed PL blueshift upon anneal [15].

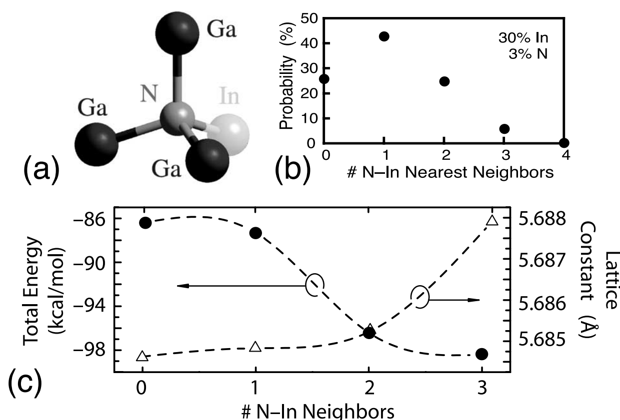

FIG. 1. (a) The chemical environment around N is characterized by the ratio of Ga:In nearest neighbors. (b) The probability of finding a given number of In nearest neighbors to any Group V lattice site is plotted for a random alloy with 30% In. (c) The variation of lattice constant and total energy is calculated as a function of N chemical environment.

Figure 2(a) shows N K-edge XANES spectra taken from 3000 Å thick samples of as-grown and annealed GaInNAs, as well as from a GaNAs reference sample. The GaNAs spectrum shifts $\sim$0.2–0.3 eV when In is added and an additional $\sim$0.1 eV after annealing. Intensity changes are also observed between 400.5–401.5 eV, as well as at the edge peak.

Interpretation of the XANES spectra requires accurate band structure calculations to determine the joint DOS for the probed transition, which is the experimental quantity measured by XANES [16]. The joint DOS is dominated by the DOS of the final state in this case, since the initial state (the N 1s core-level) is sharp in energy. The final state lies within the empty 2p states on the N atom where the excitation took place, thus the spectra are properly described by the N-2p PLDOS.

Simulated XANES spectra for the different model structures, shown in Fig. 2(b), were obtained by convolving the N-2p PLDOS by a 0.35 eV (FWHM) Gaussian to account for the finite monochromator resolution and for lifetime broadening. The PLDOS were calculated relative to the Fermi levels in each model and were shifted to match the absolute edge energy. Relative offsets between the spectra were determined from calculated core-level shifts (Δc) and conduction band offsets (CBO). The CBO were taken directly from band structure calculations, since the model structures are nearly identical and therefore the average bulk local potentials can be assumed to be the same [17]. In practice, the core-level shifts dominate the band offsets by 2 orders of magnitude anyway. Core-level shifts are calculated in the initial state approximation by computing the average electrostatic potential $\overline{V}$ on the N ion for each model, via

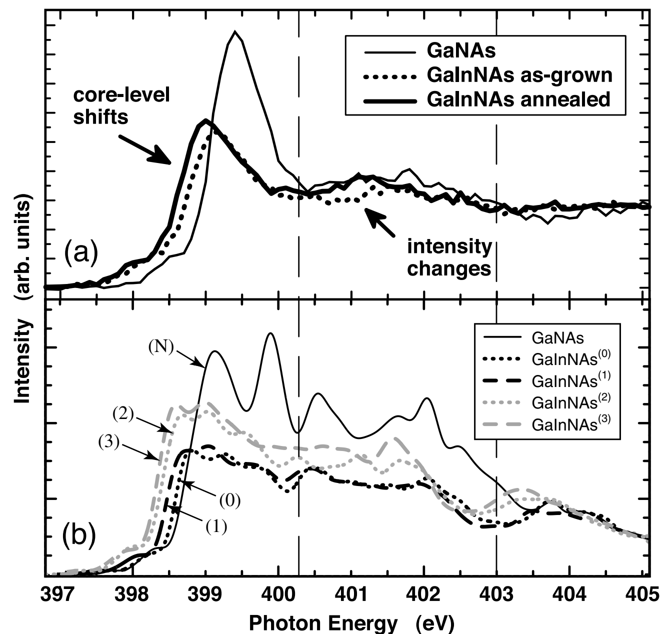

FIG. 2. (a) Measured N K-edge XANES spectra, and (b) simulated spectra from N PLDOS.

$$\overline{V} = \int V(\mathbf{r})\rho_{\text{test}}(|\mathbf{r} - \mathbf{R}_{\text{N}}|)\, d^3\mathbf{r}, \qquad (1)$$

where $V(\mathbf{r})$ denotes the potential throughout the unit cell and ρ_{test} is a normalized test charge placed a distance $|\mathbf{r} - \mathbf{R}_{\text{N}}|$ from the N center at $\mathbf{R}_{\text{N}}$. Then,

$$\Delta c = (\overline{V}_2 - E_{\text{Fermi},2}) - (\overline{V}_1 - E_{\text{Fermi},1}), \qquad (2)$$

with $\overline{V}_i$ referenced to the respective model's Fermi level.

Figure 2(b) shows that increasing the degree of N—In bonding shifts the N *K*-edge to lower energies. In addition, the Δc calculated between GaNAs and $\text{GaInNAs}^{(0)}$ is negligible, indicating that first nn bonding is the critical parameter in determining the shift. Thus, the shifts observed in Fig. 2(a) are due to In segregation toward N. The relation between nn bonding and Δc can be understood through the traditional theory of chemical shift in XANES spectra: the modification of the core potential resulting from a perturbation of the screening potential. The N—In bond has a greater electronegativity (χ) difference than the N—Ga bond, which causes N to extract more charge from In than from Ga ($\chi^{\text{In}} = 1.78$, $\chi^{\text{Ga}} = 1.81$, $\chi^{\text{N}} = 3.04$). The additional negative charge around N reduces its core-level ($1s$) binding energy and shifts the spectrum to lower energies. In fact, our simulations show increasing charge localization on N when bonded to more In atoms, causing a progressive increase in polarity of the N—In bond.

By comparing quantitatively the measured and calculated shifts in Figs. 2(a) and 2(b), we conclude that our as-grown material is nearly random in configuration. The observed shift of ~0.2–0.3 eV between GaNAs and as-grown GaInNAs, and the additional ~0.1 eV shift after RTA, is consistent with a distribution of bonds dominated by $\text{GaInNAs}^{(1)}$ before annealing and $\text{GaInNAs}^{(3)}$ after annealing. Figure 1 shows that this corresponds to the random configuration before annealing and the thermodynamic configuration after annealing. This result is not surprising, as our low-temperature MBE growth promotes a kinetic product, while increased thermal dosing during RTA moves the material toward equilibrium. A previous theoretical study using Monte Carlo simulations also predicted a thermodynamically preferred configuration favoring N—In_3Ga clusters, but did not consider the effects of annealing or high In content [6].

While nn bonding directly impacts the spectrum shift, finer details of the bonding appear as differences in the precise edge shape (i.e., the oscillations above the edge). The increases in intensity observed around 401 eV and at the edge peak both can be attributed to increased numbers of N—In bonds, as shown in Fig. 2(b). Our simulations show strong oscillations due to the artificial long-range periodicity introduced by the supercells and also finite **k**-point sampling. While averaging several supercells may better model the alloy effects, a previous study has shown this to have only a minor effect on the DOS [18]. Additional effects such as second nn interactions and N clustering could affect the spectra to second order, but we have not considered these effects here.

In addition to N XANES, we also measured the nn radial distribution function (RDF) around In for as-grown and annealed 80 Å GaInNAs quantum well samples. The results, shown in Fig. 3(a), were obtained by *k*-space filtering and taking the Fourier transform of In *K*-edge EXAFS spectra. The RDFs for both as-grown and annealed material show a dominant In—As peak at ~2.25 Å and a smaller shoulder at shorter bond lengths. The shoulders correspond to the In—N bond, whose precise length is shown by simulations to depend on the number of Ga atoms around N [see Fig. 3(b)]. The sharp curves in Fig. 3(b) show the distribution of In bond lengths calculated for the different model crystal structures. Simulated RDFs were then obtained and fit to the experiments by convolving the bond length distributions with a mixed Gaussian-Lorentzian function and assuming that annealing drives the material from a distribution with mostly $\text{GaInNAs}^{(1)}$ to mostly $\text{GaInNAs}^{(3)}$. The In—N shoulder in the RDF becomes more prominent after annealing because the number of In—N bonds increases

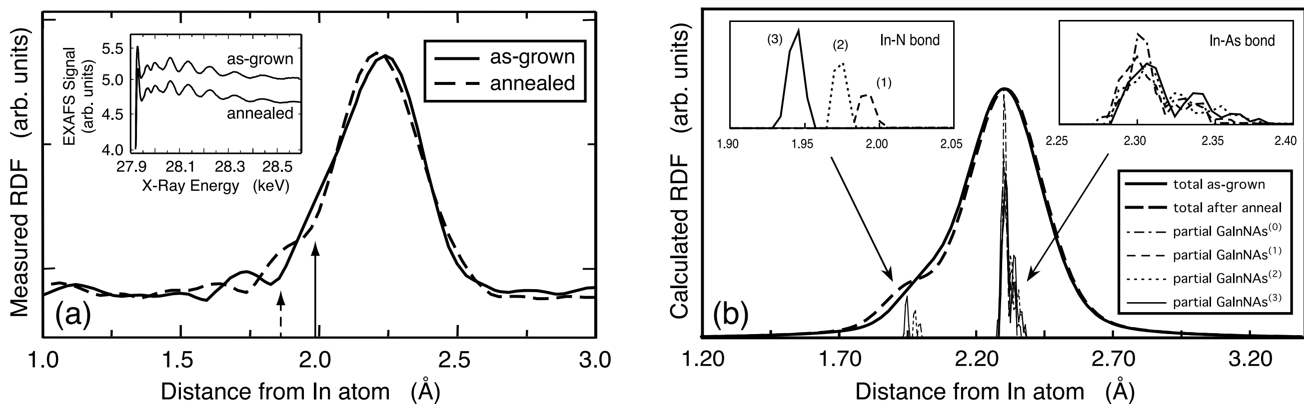

FIG. 3. (a) Measured In first nn RDF, from *K*-edge EXAFS (inset). Arrows indicate the In—N bond. (b) Simulated RDFs, calculated from bond-length distributions in the model structures. The insets show closeup views of the component peaks.

and also because the peak radius shifts further from the center of the overwhelming In — As peak. There is an excellent match between the simulation and experiment, and again we conclude that annealing increases the degree of N — In bonding.

Finally, "fat bands" analysis, where the band structure is decomposed into contributions from various atomic orbitals [19], was performed to further understand the relationship between the arrangement of N — In(Ga) bonds and the band gap shift/annealing behavior. Qualitatively, the band structure of GaInNAs and GaNAs (with relatively high N content $\gtrsim 1\%$) is similar to that of GaAs (or InGaAs), with a notable exception [15]. As in GaAs/InGaAs, near Γ, a valence band rich in As-$4p$ states forms, with a conduction band rich in Ga-$4s$ and In-$5s$ states forming $\sim$1–1.5 eV higher in energy. For the nitrides, a new conduction band forms between these two bands, $\sim$0.7–1.0 eV below the original conduction band, that is characterized by s-orbital interactions between N and its four nn's. The N concentration is high enough that these semilocalized states form a band by interacting weakly through the electron density of the matrix. The upper conduction band is dominated by Ga(In) — As bonding far from the N atoms. The dispersion of the N band is more than 1 eV in bandwidth and is similar in shape to the GaAs or InGaAs conduction band. As more In atoms bond to N in GaInNAs, an appreciable amount of In-$5s$ contribution from the upper conduction band shifts to the lower N band, and the N band simultaneously increases in energy. Since the N band, which determines the band gap, is dominated by N nn bonding, we can understand why the band gap increases when the number of N — In nn's increases. Total energy calculations show that, when both Ga and In are bonded to N, the Ga — N bond is stretched further from equilibrium than the In — N bond. Additionally, the Ga — N bond is further stretched when fewer In atoms are bonded to N. In this way, the degree of valence electron interaction between the atoms is modulated by the Ga:In ratio. When the N conduction band is dominated by N — In bonding, the band gap is larger since the reduced bond stretching leads to stronger interatomic interactions. Details of the atomic relaxations in each environment lead to a nonlinear variation of the band gap with number of N — In nn's [15].

Because of the importance of the In-$5s$ contribution to the blueshifted N band, it is possible that the same mechanism that blueshifts the PL upon annealing also contributes somewhat to increasing the PL efficiency by creating additional N — In "active sites." Of course other factors related to annealing, such as the removal of point defects, are important in improving PL efficiency as well. We are currently working on temperature-dependent absorption measurements to elucidate the details of our proposed band structure model and its implications for optical emission, but it is at least consistent with experimental results published by other groups [7,20].

In conclusion, we have found that annealing GaInNAs drives the creation of additional N — In bonds beyond what is statistically expected for a random alloy, but consistent with the thermodynamically predicted most stable structure. Our as-grown MBE material has a nearly random distribution of N and In atoms, while annealed material contains an increased number of N — In bonds. This nearest neighbor reconfiguration is responsible for a large part of the PL blueshift observed after annealing, and probably has some role in the increase of PL efficiency as well. The N — In bond contributes significantly to a low-energy conduction band responsible for the reduced band gap of this material, explaining the observed behavior.

Financial support was provided by DARPA and ONR through the Optoelectronics Materials Center, Contract No. MDA972-00-1-0024, DARPA/ARO, Contract No. DAAG55-98-1-0437, and ONR Contract No. N00014-01-1-0010. V. L. also thanks the Hertz Foundation for financial support. NPACI provided supercomputer time at SDSC and TACC. The authors thank I. Tanaka, M. Yamada, T. Uruga, and S. Komiya for useful discussions.

*Electronic address: vlordi@snow.stanford.edu
†Present address: LLNL, Advanced Detector Group, L-418, Livermore, California 94550-9234.

[1] M. Kondow *et al.*, Jpn. J. Appl. Phys. **35**, 1273 (1996).
[2] J. S. Harris, Jr., Semicond. Sci. Technol. **17**, 880 (2002).
[3] S. G. Spruytte *et al.*, J. Appl. Phys. **89**, 4401 (2001).
[4] S. G. Spruytte, Ph.D. thesis, Stanford University, 2001.
[5] R. Magri and A. Zunger, Phys. Rev. B **44**, 8672 (1991).
[6] K. Kim and A. Zunger, Phys. Rev. Lett. **86**, 2609 (2001).
[7] P. J. Klar *et al.*, Phys. Rev. B **64**, 121203(R) (2001).
[8] S. Kurtz *et al.*, Appl. Phys. Lett. **78**, 748 (2001).
[9] V. Gambin *et al.*, J. Cryst. Growth (to be published).
[10] S. G. Spruytte *et al.*, J. Cryst. Growth **227–228**, 506 (2001).
[11] S. Friedrich *et al.*, Rev. Sci. Instrum. **73**, 1629 (2002).
[12] G. Kresse and J. Hafner, Phys. Rev. B **47**, 558 (1993); **49**, 14 251 (1994); G. Kresse and J. Furthmüller, Comput. Mater. Sci. **6**, 15 (1996); Phys. Rev. B **54**, 11 169 (1996).
[13] D. Vanderbilt, Phys. Rev. B **41**, 7892 (1990).
[14] H. J. Monkhorst and J. D. Pack, Phys. Rev. B **13**, 2339 (1976).
[15] V. Lordi (to be published).
[16] J. Stöhr, *NEXAFS Spectroscopy* (Springer-Verlag, Berlin, 1992).
[17] C. G. Van de Walle and R. M. Martin, Phys. Rev. B **35**, 8154 (1987).
[18] E. D. Jones *et al.*, Phys. Rev. B **60**, 4430 (1999).
[19] O. Jepsen and O. K. Andersen, Z. Phys. B **97**, 35 (1995).
[20] W. Shan *et al.*, Phys. Rev. Lett. **82**, 1221 (1999).